

Chapter 5

Self-compression of Intense Femtosecond Pulses in Gas-filled Hollow-core Waveguides

One surprising experimental result that came out of my research on high harmonic generation was the observation of temporal compression of the 800 nm driving pulse after propagating in a hollow-core waveguide filled with low-pressure argon at ionizing intensities. Unlike other standard pulse compression techniques, no subsequent dispersion compensation was used. Typically, pulse compression is accomplished by broadening of the spectrum of the pulse through nonlinear self-phase modulation. This broadened pulse bandwidth can then be compressed to a shorter pulse by appropriate dispersion compensation. Self-phase modulation of the pulse can be done by propagation through an optical fiber[53, 73] or a gas-filled hollow waveguide[54] at non-ionizing intensities and dispersion compensation is provided by prisms, gratings, or chirped mirrors to create a negative group velocity dispersion. These schemes have been employed to compress pulses to under 4 fs pulse duration[82]; however, such techniques are lossy and can be quite complicated. Furthermore, all previous pulse compression schemes have been limited to sub-millijoule pulse energies due to the damage threshold of the fibers or ionization of the gas. The use of ionization to broaden the spectrum of a pulse for compression has been previously considered theoretically.[72] However, the compression also depended on negative group velocity dispersion compensation.

5.1 Experimental Results

In the experiment, light from a Ti:sapphire amplifier producing ~ 30 fs near-transform limited pulses with 2.5 mJ pulse energies at 1 kHz was focused into a 2.5 cm long, 150 micron inner-diameter hollow waveguide filled with low pressure argon. The spot diameter of the laser mode at the entrance of the waveguide was $\sim 85 \mu\text{m}$ FWHM and the energy throughput of the waveguide was $\sim 60\%$ with no gas. The focusing region before and after the waveguide was held under vacuum to prevent any additional nonlinear effects. The pulse was characterized before and after the waveguide using second-harmonic frequency-resolved-optical-gating (SHG-FROG).[74] All FROG measurements were deconvolved using commercial software from Femtosoft Technologies (FROG Version 3.03) to an error of $< 1\%$ for a 256×256 sampling grid. The spectral marginals for each measurement agree with the experimentally measured spectra to within 5%. After exiting the waveguide, the pulse passes through a $250 \mu\text{m}$ thick sapphire window and a 1 mm thick fused silica beam splitter in the FROG setup. The total dispersion of these elements corresponds to a group velocity dispersion of 61 fs^2 and a third-order dispersion of 40 fs^3 at a center wavelength of 760 nm, which would change the pulse duration at most by 3 fs, not enough to significantly affect the experimental results. Also, the material gives a positive group velocity dispersion, which would not explain pulse compression by the typical schemes. The pulse shape after the fiber without gas is the same as the input to within our measurement resolution.

The intensity in the waveguide, approximately 10^{15} W/cm^2 , is high enough to completely doubly ionize the argon gas by the peak of the pulse (for a 30 fs duration pulse). This rapidly changing ionization during the pulse results in an index of refraction that decreases with time, causing a blue shift of the overall laser spectrum. The spectra at the exit of the waveguide with varying pressures of argon is shown in figure 5.1. Pressures as low as 1 Torr result in significant blue shift and spectral broadening and blue shifts of up to $\sim 50 \text{ nm}$ are observed. Figure 5.2 shows the deconvolved FROG measurements of the temporal pulse shape after the waveguide

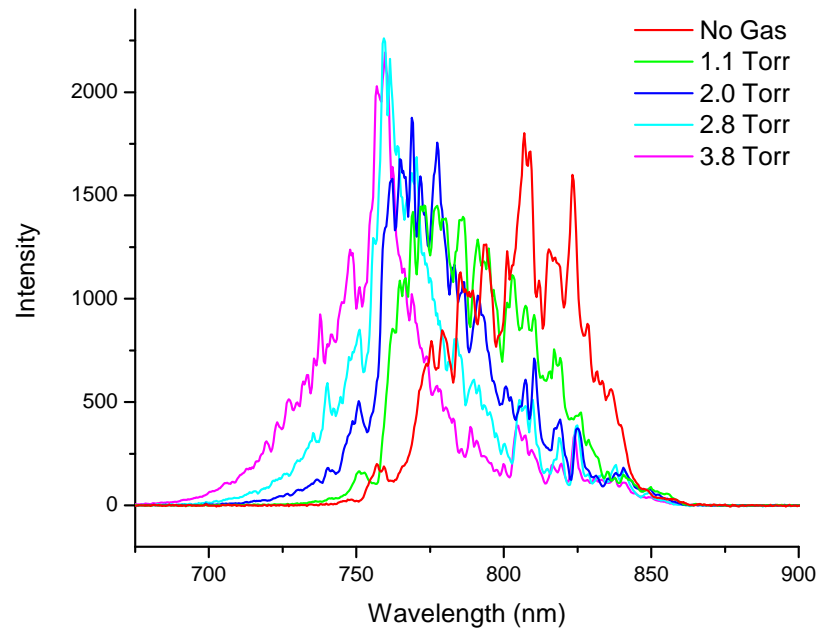


Figure 5.1: Spectra taken after the 2.5 cm long, 150 μm diameter waveguide with different Ar pressures.

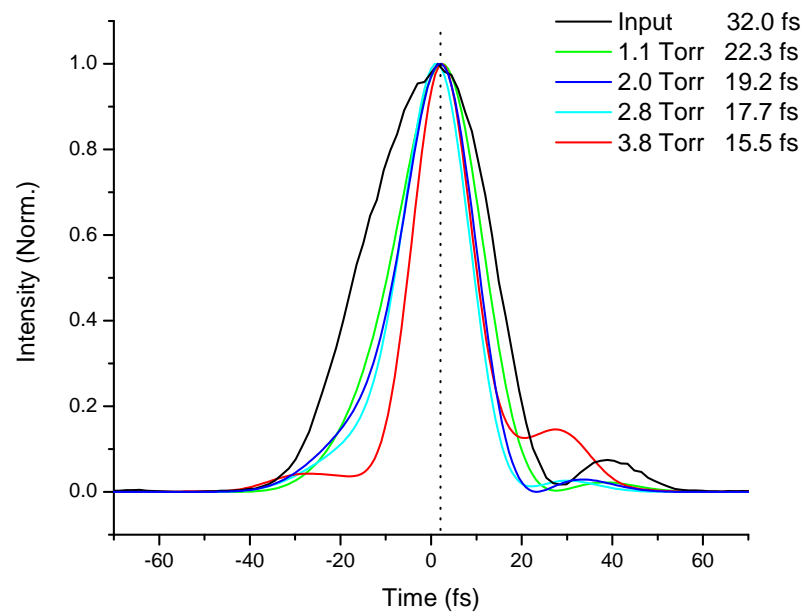


Figure 5.2: Deconvolved FROG measurements of the temporal pulse shape before and after the waveguide with different Ar pressures for an initial pulse of 32 fs. The pulse FWHM for the different measurements are indicated.

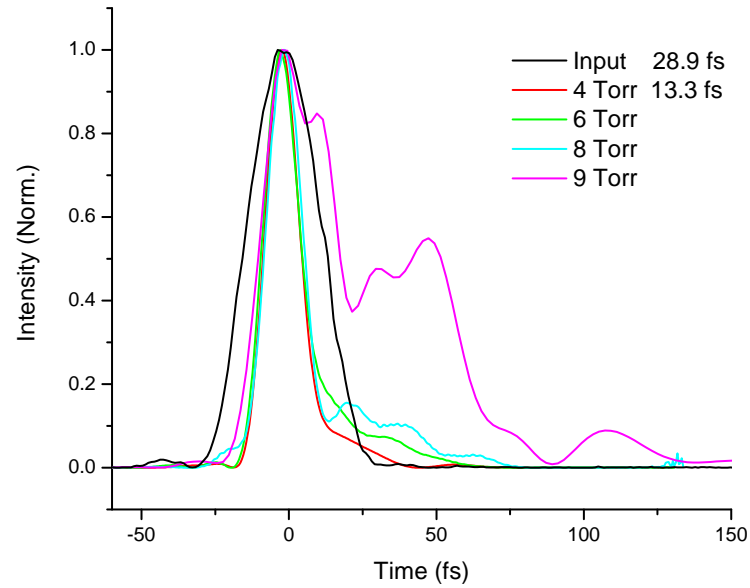


Figure 5.3: Deconvolved FROG measurements of the temporal pulse shape before and after the waveguide with different Ar pressures for an initial pulse of 29 fs. At 4 Torr, the final pulse duration is 13.3 fs FWHM. From [78].

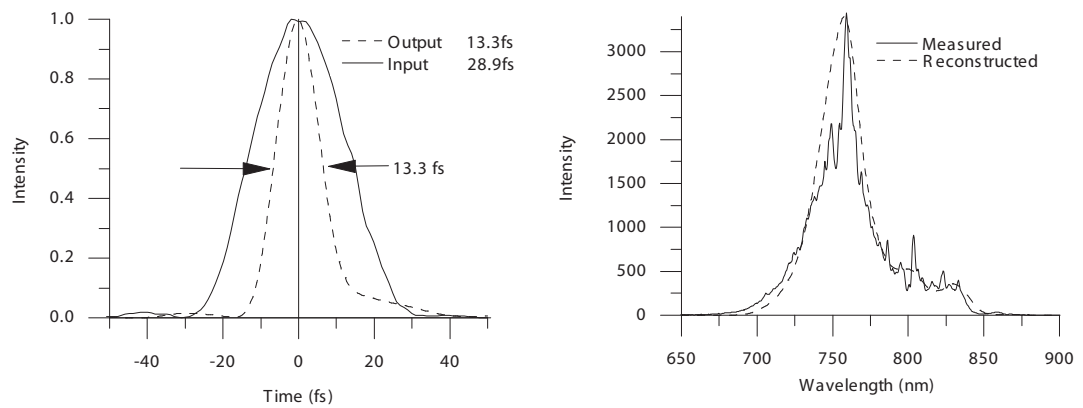


Figure 5.4: Comparison of the measured spectrum with the spectrum from FROG measurement deconvolution.

for different argon pressures. With only 1 Torr of argon, the initial pulse width of 32 fs has been drastically reduced. As the pressure is increased, the pulse width decreases to 15.5 fs at 4 Torr. Figure 5.3 shows the results for an input pulse of 29 fs duration. At 4 Torr, the final measured pulse duration is 13.3 fs. As the pressure is increased, the pulse duration remains relatively constant until 9 Torr, at which point the pulse begins to break up. The deconvolved spectrum from the FROG and the experimentally measured spectrum are shown in figure 5.4 for the 13.3 fs pulse. The excellent agreement between the two indicates that the measurement has high accuracy and is self-consistent. The spectral bandwidth can support an 11 fs transform-limited pulse. Both the input and compressed pulses are near-transform limited, within 20% of the time-bandwidth product. The power exiting the waveguide is reduced by $\sim 5\%$ with 4 Torr of Ar compared with no gas in the waveguide, while at 8 Torr, the loss is 10%. Also, the spatial mode after the waveguide remains good at low gas pressures. Using a larger diameter, 230 μm waveguide, the pulse is only compressed to 24 fs from a 30 fs duration input. When the waveguide is replaced with a 1 cm diameter gas-filled cell, there is negligible compression of the pulse.

5.2 A New Mechanism for Pulse Compression

Conventional 1-D pulse propagation models[1, 13] such as those used to calculate self-phase modulation in optical fibers, microstructured fibers, or gas-filled hollow waveguides, fail to explain the experimental self-compression observed. The blue-shift and broadening of the spectrum can be explained by self-phase modulation from the changing plasma index; however, this will not alter the temporal envelope. The dispersion of the low-pressure gas, the plasma, or the waveguide is too small to affect the temporal shape as well. Higher-order nonlinear effects can cause self-steepening of the pulse which can reshape the trailing edge, but will not shorten the pulse in time.

Table 5.2 summarizes the potential 1-D pulse shaping mechanisms and the characteristic propagation length over which they become significant for our conditions.[13] The dispersion

length is given by:

$$L_{dis} = \frac{T^2}{\left| \frac{d^2k}{d\omega^2} \right|}, \quad (5.1)$$

where T is the pulse duration (1/e intensity) and $k = \omega n/c$. For a 30 fs pulse FWHM, $T = 18$ fs. The dispersion length is the length over which the pulse duration would approximately double due to group velocity dispersion (GVD). Self-phase modulation becomes important when the spectral broadening is on the order of the spectral width of the initial pulse. The amount of SPM broadening is given approximately by $d\phi(\omega)/dt$ or $\sim \Delta\phi_{NL}/T$ where $\Delta\phi_{NL} \sim n_2 I \omega L/c$. The bandwidth of the input pulse is approximately $1/T$. Therefore, SPM is significant when $\Delta\phi_{NL} \sim 1$ and the effective length is given by:

$$L_{SPM} = \frac{c}{\omega n_2 I}. \quad (5.2)$$

Another nonlinear mechanism is self-steepening of the pulse. The self-steepening process depends on the nonlinear group index which is defined as $n_2^{(g)} = n_2 + \omega \frac{dn_2}{d\omega}$. In our case, the assumption $n_2^{(g)} \approx n_2$ is valid. The effective length over which self steepening is significant is given by:

$$L_{SS} = \frac{cT}{n_2^{(g)} I}. \quad (5.3)$$

Lastly, the time-varying index due to ionization during the pulse also affects the pulse spectrum. The plasma index is given by:

$$n_p = \sqrt{1 - \frac{\omega_p^2}{\omega^2}} \simeq 1 - \frac{\omega_p^2}{2\omega^2}, \quad (5.4)$$

where ω_p is the plasma frequency given by: $\omega_p^2 = N_e e^2 / m \epsilon_0$, e and m are the electron charge and mass, and N_e is the electron density. Because the electron density is increasing in time during the leading part of the pulse, the plasma index is also changing during the pulse. In this way, the plasma index acts like the nonlinear index, $n_2 I$, the difference being that it only decreases during the pulse, instead of increasing and decreasing over the duration of the pulse. Therefore, the spectrum predominately broadens to shorter wavelengths. The length over which the effective nonlinear index from the plasma will affect the spectrum from self-phase modulation is given by $L_{PlasmaSPM} = c/\omega n_p$ and the effective self-steepening length given by $L_{PlasmaSS} = cT/n_p$.

Mechanism	Length scale	Distance
Waveguide GVD	$L = \frac{T^2 a^2 \omega^3}{u_{1c}^2}$	14 m
Gas GVD	$L = \frac{T^2 2\pi c^2}{\lambda^3 a^2 n^2}$	1.5 km
Plasma GVD	$L = \frac{T^2 c \omega^3}{\omega_p^2}$	1.4 m
Gas SPM	$L = \frac{c}{\omega n_2 I}$	10 cm
Gas self-steepening	$L = \frac{c T}{n_2^{(g)} I}$	4 m
Plasma SPM	$L = \frac{2\omega c}{\omega_p^2}$	2 mm
Plasma self-steepening	$L = \frac{2T c \omega^2}{\omega_p^2}$	1 cm
Plasma defocusing	$L = \frac{1}{2} k \omega^2 = \frac{2\omega c}{\omega_p^2}$	1.5 mm

Table 5.1: Table of possible pulse shaping mechanisms that involve only 1-D propagation effects and the propagation length over which they become significant. The conditions used in the calculation are 4 Torr of Ar in a 150 μm diameter hollow waveguide. The gas terms were calculated for no ionization, and the plasma terms were calculated for 200 % ionization.

A 1-D propagation model was performed by Tempea et al.[72] for similar conditions: pulse intensities of 7×10^{14} to 1.5×10^{15} W/cm², 125 μ m inner-diameter hollow waveguide, 20 fs input pulse, and argon pressure of ~ 0.5 Torr. They found significant spectral broadening to shorter wavelengths for long propagation lengths (90 cm) with a positive chirp on the output pulse, but did not observe any temporal compression from their model.

Since 1-D nonlinear wave propagation cannot explain our experimental observations and because the waveguide is necessary to achieve pulse compression, a 3-D propagation model was employed. Propagation of the laser pulse in the waveguide was modelled by numerical solution of the 3-D scalar wave equation. This model was developed by Ivan Christov and is described in more detail in Ref. [18]. The model takes into account the dispersion from the transient plasma, power dissipation from ionization, and dispersion due to the neutral gas at each radial position in the waveguide as a function of time. The 3-D diffraction by the waveguide is included and automatically accounts for the waveguide dispersion. The waveguide loss was also measured experimentally and incorporated into the model.

The theoretically predicted pulse durations and spectra as a function of pressure are shown in Figs. 5.5 and 5.6. The model is in excellent agreement with experimental data, predicting that the pulse undergoes temporal reshaping that reduces the pulse width from 30 fs to approximately 13 fs with increasing pressure, and that the minimum pulse duration is obtained around 4 Torr. The leading edge of the pulse also steepens in time, accompanied by a longer trailing edge that develops a shoulder as the pressure is increased - again in very good agreement with experiment. The model also predicts less compression for larger diameter waveguides and little or none for the case of no waveguide, as is the case experimentally. Finally, the corresponding pulse spectra blue shift and increase in bandwidth due to the combined effects of rapidly changing plasma index and self-phase modulation are also in good agreement with experiment. At high pressures above 8 Torr, the pulse splits and the spectrum develops a large long-wavelength wing, also observed experimentally. The only adjusted parameter in the calculations to obtain agreement was the input diameter of the focused laser mode into the

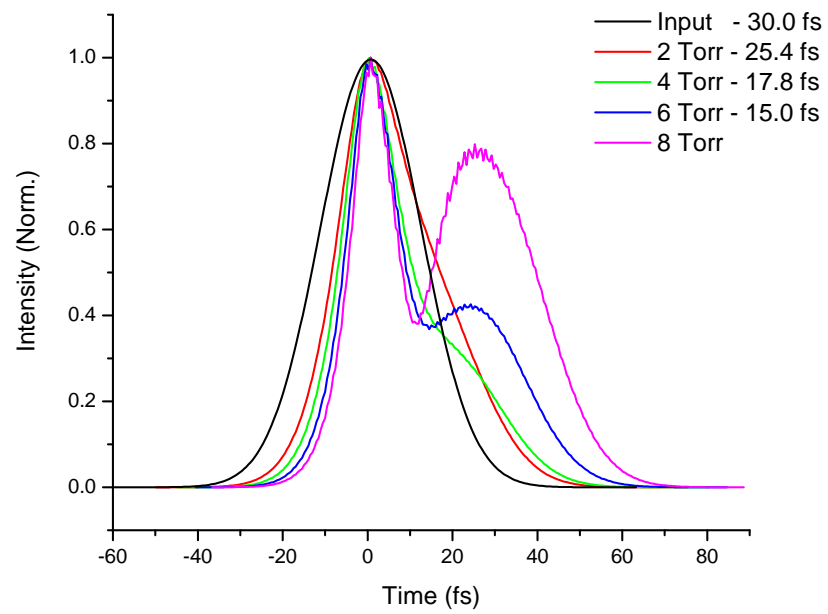


Figure 5.5: Theoretical calculation of temporal pulse shape after the waveguide with different Ar pressures for an initial pulse duration of 30 fs using the 3-D propagation model. The pulse FWHM are indicated.

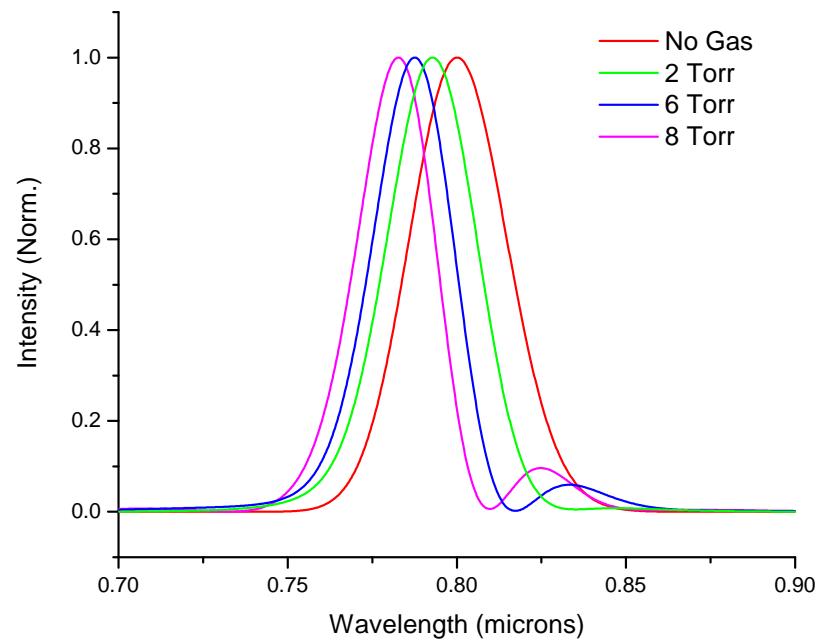


Figure 5.6: Theoretical calculation of the pulse spectrum before and after the waveguide with different Ar pressures.

waveguide.

The self-compression is a result of the combined effects of plasma-induced refraction and blue shifting, diffraction of the laser beam, phase modulation due to the rapidly-changing plasma index, and guiding by the hollow waveguide. The role of plasma defocusing combined with the waveguide refocusing governs the spatial propagation and is very important in the compression process. The model shows that as the pulse begins to ionize the gas, the trailing edge of the pulse refracts from the center of the waveguide due to plasma-induced defocusing. However, this portion of the beam is then reflected back into the guide by the waveguide walls. This leads to a temporally compressed pulse with a sharp leading edge and flat temporal phase. The reshaping also leads to a small periodic oscillation in the beam diameter and pulsewidth as the pulse propagates down the waveguide. This high-field pulse reshaping process has similarities with passive mode locking of lasers using saturable absorbers - the trailing edge of the pulse is slowly depleted periodically along the waveguide due to ionization-induced defocusing, where the role of a laser resonator is replaced by the waveguide. Both experimentally and theoretically, the pulse compression process is sensitive to the initial mode coupled into the waveguide. Also, theoretically, the laser beam must be focused to a tighter focal spot diameter than the ideal $100\ \mu\text{m}$ for coupling into the lowest-order mode of $150\ \mu\text{m}$ waveguide, in agreement with our experimental observations.

A new mechanism for pulse compression that operates at laser intensities above the ionization threshold has been demonstrated both theoretically and experimentally. This technique allows compression of pulses with millijoule energies and has the advantage of minimal distortion of the laser mode, low power loss, and no need for additional dispersion compensation. It is likely to scale to higher intensities and pulse energies, making it useful for high-field science and applications.